ELSEVIER

Neurobiology of Aging 26 (2005) 1215–1227

NEUROBIOLOGY OF AGING

www.elsevier.com/locate/neuaging

Age-related alterations in white matter microstructure measured by diffusion tensor imaging

D.H. Salat[a,*], D.S. Tuch[a], D.N. Greve[a], A.J.W. van der Kouwe[a], N.D. Hevelone[a], A.K. Zaleta[a], B.R. Rosen[a], B. Fischl[a,b], S. Corkin[a,c], H. Diana Rosas[a,d], A.M. Dale[a,b,e]

[a] *MGH/MIT/HMS Athinoula A. Martinos Center for Biomedical Imaging, Building 149, 13th St., Mail Code 149 (2301), Charlestown, MA 02129-2060, USA*
[b] *MIT Artificial Intelligence Laboratory, Cambridge, MA, USA*
[c] *MIT Department of Brain and Cognitive Sciences, Cambridge, MA, USA*
[d] *MGH Department of Neurology, Boston, MA, USA*
[e] *UCSD Departments of Neurosciences and Radiology, La Jolla, CA, USA*

Received 29 April 2004; received in revised form 26 August 2004; accepted 30 September 2004

Abstract

Cerebral white matter (WM) undergoes various degenerative changes with normal aging, including decreases in myelin density and alterations in myelin structure. We acquired whole-head, high-resolution diffusion tensor images (DTI) in 38 participants across the adult age span. Maps of fractional anisotropy (FA), a measure of WM microstructure, were calculated for each participant to determine whether particular fiber systems of the brain are preferentially vulnerable to WM degeneration. Regional FA measures were estimated from nine regions of interest in each hemisphere and from the genu and splenium of the corpus callosum (CC). The results showed significant age-related decline in FA in frontal WM, the posterior limb of the internal capsule (PLIC), and the genu of the CC. In contrast, temporal and posterior WM was relatively preserved. These findings suggest that WM alterations are variable throughout the brain and that particular fiber populations within prefrontal region and PLIC are most vulnerable to age-related degeneration.

Keywords: Aging; White matter; Prefrontal; Motor; Corticospinal; Internal capsule; Myelin

1. Introduction

The aging brain exhibits an assortment of micro- and macroscopic changes that ultimately result in some degree of cognitive and functional decline. Although the majority of studies of normal aging have focused on the cerebral cortex, it is clear that cerebral white matter (WM) also exhibits various types of age-related degenerative changes. Histological studies demonstrate a decrease in myelin density and in the number of myelinated fibers [9,35]. Autopsy [35] and volumetric neuroimaging studies [12,22,28,51] suggest that WM changes are more prominent than cortical changes with aging, at least during certain segments of the age span and in certain regions of the brain. For example, prefrontal WM volume loss is disproportionately greater than cortical volume loss in this area with late aging (comparison of older adults (OA) aged 60–75 with oldest old aged >85; [51]); yet, this selectivity may not be apparent when examining changes across the adult age span [45]. Additionally, theories of brain aging suggest that association systems show significantly greater age-related alterations compared to primary sensory and motor systems [30,44]. Although patterns of accelerated cortical volumetric change have been demonstrated, the regional patterns of age-related changes in brain WM are unknown. Specifically, it is unclear whether changes in brain WM are global in nature, or are accelerated in specific vulnerable regions or circuits of the brain.

* Corresponding author. Tel.: +1 617 726 5486; fax: +1 617 726 7422.
E-mail address: salat@nmr.mgh.harvard.edu (D.H. Salat).

0197-4580/$ – see front matter © 2004 Published by Elsevier Inc.
doi:10.1016/j.neurobiolaging.2004.09.017

Recent neuroimaging studies find differing results depending on the technique employed. For example, studies show that prefrontal WM T2 signal alterations do not differ appreciably compared to signal alterations in the temporal lobe [4], suggesting that there is no difference in the age-related vulnerability of frontal and temporal WM. In contrast, volumetric studies demonstrate that prefrontal WM and cortical change are greater than changes in the temporal lobes [14,28,45], indicating that age-related changes are different from those of neurodegenerative diseases such as Alzheimer's disease (AD).

Few longitudinal studies exist, but such studies are critical for deciphering regional brain vulnerability. Recent longitudinal studies using voxel-based techniques to examine MR signal characteristics suggest that WM is somewhat preserved in visual areas, such as occipital regions [16] and that age-related change is lateralized, with greater alterations in the left hemisphere [16]. Longitudinal studies examining WM morphometry demonstrate widespread changes throughout the brain across four years in older adults [47].

Traditional volumetric imaging studies are limited in that they typically employ a 'region' or 'volume of interest' approach which cannot specify the regional patterns of WM change beyond a predefined and somewhat arbitrary area of interest. This limitation is compounded by the fact that the orientational organization of specific WM bundles in the brain is highly complex, appearing as a single tissue mass of mostly homogeneous signal intensity on a typical T1-weighted volumetric scan. Voxel-based techniques are less subjected to such regional limitations [47]; yet, recent advances in diffusion tensor imaging (DTI) can now robustly differentiate among distinct WM structures, and thus these methods could be useful to study the regional nature of age-related reductions in WM integrity.

DTI contrast is based on the molecular diffusion of water, and this diffusion is influenced by microstructural factors including myelin density, membrane intactness, and possibly other fiber components [6]. As such, the DTI signal is an indirect measure of various aspects of tissue integrity yet potentially sensitive measure of alterations in tissue properties. A metric of WM integrity, 'fractional anisotropy' (FA), is computed from the diffusion properties within a voxel. This metric is high in regions of the brain with highly restricted diffusion, such as regions of the brain with highly organized myelinated structure (e.g., the corpus callosum, CC), and lower in regions of the brain with less organized structure (e.g., the intersection between the callosal fibers and the superior longitudinal fasciculus). Alterations in the microstructural environment, such as a change in tissue density, would affect this measurement. Similar metrics have been used to detect WM pathology in several neurological and psychiatric conditions including multiple sclerosis [13,21,48,63], stroke and ischemia [38,56,65], and schizophrenia [1,24,31–33,64]. The signal abnormality in the DTI scan is presumed to reflect alterations in tissue properties, including decreased myelination and/or a decreased number of myelinated nerve fibers. Thus, FA could provide a useful metric of commonly measured histological properties. Importantly, a number of studies have demonstrated that DTI measures are altered in abnormal WM that appears to be normal on conventional MR images (e.g., [63]).

Prior studies using DTI have demonstrated age-related changes in anisotropy in the genu of the corpus callosum [42], anterior WM [37,41], and periventricular WM [36]. Regional anisotropy or diffusivity correlated with cognitive abilities in studies of normal aging [37] and with disease severity in AD [7], demonstrating the clinical relevance of this metric towards characterizing age-related neurodegenerative disorders. Studies have only recently employed DTI measures of FA to detect whole brain patterns of WM alterations with aging [23,36]. These studies found that anisotropy was decreased in a variety of neural regions, particularly in prefrontal WM. Still, few studies have examined age-related WM alterations in multiple brain areas to directly examine how changes in FA relate to commonly held theories of brain aging.

The current study had three primary aims. The first was to determine whether age-related WM changes are ubiquitous throughout the brain or are accelerated in prefrontal WM relative to WM associated with other cortical lobes. The second aim was to ask whether alterations in prefrontal WM are homogeneous throughout the lobe or are selective to particular regions. The third aim was to examine whether WM associated with primary sensory or motor circuits, such as occipital WM and WM in the internal capsule, was relatively preserved compared to WM in other areas. The use of advanced whole-head DTI sequences reduced common artifacts in diffusion images such as eddy current distortion. These images were examined using complimentary region-of-interest (ROI) and whole-brain analysis techniques. The findings suggest that alterations in prefrontal WM are relatively accelerated compared to temporal WM, that WM changes are particularly accelerated in anterior and ventromedial regions of prefrontal cortex as compared to other prefrontal regions, and that WM of visual cortex is spared, yet motor projections are vulnerable to age-related degeneration.

2. Methods

2.1. Participants

Diffusion tensor images were obtained from 38 participants aged 21–76 years (18 M/20 F). Older adults (60 years and older; 6 M/8 F) were recruited through the Harvard Cooperative on Aging. Young (YA; 21–39 years; 6 M/9 F) and middle-aged (MA; 40–59 years; 6 M/3 F) adults were recruited from the Massachusetts Institute of Technology and Massachusetts General Hospital communities. YA, MA, and OA were matched for education. OA and MA were screened for dementia using the Mini Mental Status Exam-

Table 1
Participant demographics

Group	*N*	Age	Education	MMSE[a]
YA[b]	15	26.3 (21–37)	18.4 (16–29)	N/A
MA[c]	9	51.8 (42–59)	16.0 (12–21)	29.5[d] (28–30)
OA[e]	14	70.9 (65–76)	17.0 (12–22)	29.4[f] (28–30)

Data presented as mean and range where applicable.
[a] MMSE: Mini Mental State Examination.
[b] YA: young adults.
[c] MA: middle-aged adults.
[d] Data unavailable for one participant.
[e] OA: older adults.
[f] Data unavailable for four participants. These four participants were screened using TICS-M.

ination (MMSE) [19] (Table 1). Four OA did not complete the MMSE and were instead screened for dementia using the Telephone Interview for Cognitive Status (TICS/TICS-m; [8,17,34]). All participants provided written informed consent, and completed an extensive health-screening questionnaire. Participants were healthy and excluded if they had a history of neurological or psychiatric disorder, or serious cardiovascular disease. Of the 38, 2 had controlled high blood pressure. Two others had a history of concussion. Data were analyzed without these participants and we concluded that their data did not substantially affect the reported findings. These participants were therefore included in the analyses.

2.2. MRI

All participants received a high-resolution whole-head DTI scan (Siemens, Erlangen Germany, 1.5 T Sonata System; TR = 14.4 s, TE = 81 ms, slice thickness = 2 mm isotropic, 60 slices total, acquisition matrix 128 mm × 128 mm (FOV = 256 mm × 256 mm), 5/8 partial Fourier, 6 averages, 6 non-collinear directions with *b*-value = 700 s/mm^2, and 1 image, the T2 weighted 'low*b*' image, with *b*-value = 0 s/mm^2). The effective diffusion gradient spacing was Δ = 37 ms and the bandwidth was 1445 Hz/pixel. Images were collected oblique axial with a total scan duration of 11 min 31 s. The DTI acquisition used a twice-refocused balanced echo, developed to significantly reduce eddy current distortions [46]. Head motion was minimized by the use of tightly padded clamps attached to the head coil.

2.3. Image analysis

DTI data were processed using a multistep procedure to achieve the following: (a) motion and residual eddy current distortion correction; (b) calculation of FA maps from the corrected volume; (c) spatial transformation of each participant's low*b* volume (the volume from the diffusion acquisition with no diffusion weighting (T2-weighted), providing greater structural contrast) to a low*b* template in normalized space based on MNI/Talairach space created by our group from similar diffusion datasets; (d) resampling of the FA map using the transformation created by step (c); (e) manual ROI measurements of FA values on the spatially normalized data of each participant; (f) creation of two additional atlas transformations, one using regional landmarks for fiducially based volumetric registration and the other using a segmentation of WM from the low*b* volume as the registration volume; (g) spatial smoothing and voxel-based calculation of group statistics on spatially normalized data. Each of these steps is described in detail below.

2.4. Preprocessing

For data processing, we used diffusion tools developed at the Martinos Center as well as tools available as part of the Freesurfer (http://surfer.nmr.mgh.harvard.edu) and FSL (http://www.fmrib.ox.ac.uk/fsl) processing streams. The low*b* structural volume was collected using identical sequence parameters as the directional volumes with no diffusion weighting, and was thus in register with the final diffusion maps. This low*b* volume was used for all registration, thus avoiding multiple registration steps of the DTI data to additional image volumes. Each directional volume from the diffusion dataset was resampled to the low*b* image to correct for remaining eddy current distortion, as well as to correct for participant motion. This procedure used the 12-parameter affine mutual information cost function transformation procedure in FMRIB's Linear Image Registration Tool (FLIRT) available through the FSL analysis stream [25,26,53,54]. The diffusion tensor was calculated for each voxel in the volume using a least-squares fit to the diffusion signal [5]. The fractional anisotropy metric was derived from the diffusion tensor as previously described [43]. To exclude the influence of cerebrospinal fluid (CSF), voxels with a trace image value of above 6 μm^2/s were set to 0 and were not included in subsequent analyses (the trace is a measure of the total amount of diffusion and is thus high in CSF). All resulting maps were resampled to 1 mm^3 resolution using trilinear interpolation (Fig. 1, top panel).

2.5. Regional analyses

All ROIs were defined on the spatially normalized low*b* volume of each individual participant using Tkmedit in the Freesurfer data processing package. Spatial normalization was performed by creating a low*b* template by first using the FSL registration tools to perform a mutual information cost function based registration between each participants low *b*-value volume and the T2 template provided by the MNI (linear 12 degrees of freedom global affine transformation) and then averaging the normalized volumes. Use of the spatially normalized low*b* volume allows for the placement of ROIs without the influence of the dependent variable (FA) or through the use of a differentially distorted scan acquisition. ROIs were placed in nine regions of interest in each hemisphere, and in the genu and splenium of the corpus

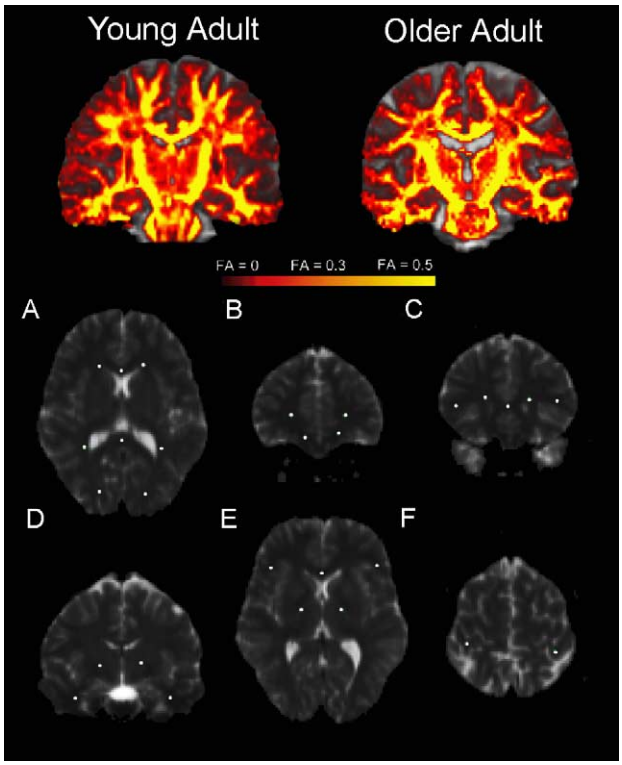

Fig. 1. FA and WM ROIs. Example of the FA metric in a coronal image of a young (top left panel) and an older adult (top right panel). The FA metric describes the restrictive microenvironment of water molecules, presumably in part due to the degree of myelination, and is therefore higher in regions of more densely packed fiber bundles that are homogeneously oriented, such as the corpus callosum. FA was sampled from nine ROIs in each hemisphere and the genu and splenium of the CC (bottom panel). The figure demonstrates the ROIs in the minimal number of images. See text for detail on ROI placement. The mean FA for all voxels in the ROI was computed excluding voxels with FA below .2 to reduce sampling of other tissue classes through partial voluming.

callosum. At least one ROI was placed in each of the four cerebral lobes and other ROIs were placed in regions important in the study of aging or age-related neurodegenerative disease (Fig. 1, bottom panel). All ROIs were placed using a standardized placement procedure using atlas-based rules with morphological landmarks in each participant's volume. All ROIs were placed by the same rater, blind to participant age and sex, and were created as a sphere with a diameter of 4 mm (totalling thirty-three 1 mm^3 isotropic voxels) to avoid arbitrary sizes of ROIs across participants. We developed anatomical definitions for each ROI with the intent to sample FA within a homogeneous region of fiber structure, to maximize sampling from the deep WM (WM approximately 3 mm or more subcortical to the gray/white border), and to avoid sampling voxels that were influenced by partial volume with gray matter or CSF. Regional values were obtained from the transformed volumes. We examined whether transformation affected the results by extracting values from the transformed volume as well as in native space in six ROIs and found that the transformed values are highly correlated with the native values (r^2 range, .8–.9) and that transformation does not result in a different pattern of statistical results. We measured global FA by segmenting the low*b* volume, resulting in a measurement that was mostly comprised of the majority of brain WM. The anterior corpus callosum was defined by maximizing the placement of the sphere within the genu of the callosum starting in the midsagittal plane and next centering in the coronal and axial planes (Fig. 1a, c, and e; Table 2); the posterior CC was defined by maximizing the placement of the sphere within the splenium of the callosum starting in the midsagittal plane and next centering in the coronal and axial planes (Fig. 1a); the posterior limb of the internal capsule (PLIC) was defined in the coronal view by using the pallidum as a regional guide and placing the sphere directly dorsomedial to the pallidum in both hemi-

Table 2
Regional definitions for region of interest analyses

Region	Definition
Anterior CC[a] (Fig. 1a, c, and e)	Maximizing the placement of the sphere within the center of the genu of the callosum
Posterior CC[a] (Fig. 1a)	Maximizing the placement of the sphere within the center of the splenium of the callosum
PLIC[b] (Fig. 1d and e)	Placed in the coronal view, placing the sphere directly dorsomedial to the pallidum
Deep frontal (Fig. 1b)	Placed using the anterior CC point to determine the axial slice, in the center of deep frontal WM diagonally from the anterior horn of the lateral ventricles
Anterior PV[c] (Fig. 1a and c)	Defined at the level of the posterior CC point in the axial plane, placed at the caps of each anterior ventricular horn
Posterior PV[c] (Fig. 1a)	Defined at the level of the posterior CC point in the axial plane, placed at the caps of each posterior ventricular horn
Medial orbitofrontal (Fig. 1b)	Defined in the coronal view at the slice where the deep frontal WM points were placed, just subcortical to WM branching into the gyrus rectus
Inferior frontal (Fig. 1c and e)	Defined in the first coronal slice where the CC joined the cerebral hemispheres anteriorly and placed in the WM subcortical to WM branching into the gyrus
Deep temporal (Fig. 1d)	Defined in the coronal slice approximately 16 mm anterior to the tip of the fornix, in the approximate center of the temporal lobe WM
Post-central (Fig. 1f)	Defined in the axial plane, just posterior to the central sulcus as the anterior border
Occipital (Fig. 1a)	Defined at the level of the posterior CC point in the axial plane, in the posterior portion of the WM within the occipital gyrus

[a] CC: corpus callosum.
[b] PLIC: posterior limb of the internal capsule.
[c] PV: periventricular.

spheres (Fig. 1d and e); deep frontal WM was defined using the anterior CC point to determine the axial slice on which to make the measurement and then placing the ROI in the center of deep frontal WM, directly diagonally from the tip of the anterior horn of the lateral ventricles in each hemisphere (Fig. 1b); anterior and posterior periventricular WM was defined at the level of the posterior CC point in the axial plane and was placed at the caps of each ventricular horn, at approximately 3 mm distance from the horn (Fig. 1a and c); medial orbital WM was defined in the coronal view at the slice where the deep frontal WM points were placed, and placed in the region just subcortical to WM branching into the gyrus rectus (Fig. 1b); inferior frontal WM was defined in the first coronal slice where the CC joined the cerebral hemispheres anteriorly and placed in the WM approximately 3 mm subcortically to WM branching into the gyrus (Fig. 1c and e); deep temporal WM was defined in the coronal slice approximately 16 mm anterior to the tip of the fornix and placed in the approximate center of the WM in the temporal lobe (Fig. 1d); post-central WM was defined in the axial plane, just posterior to the central sulcus as the anterior border (Fig. 1f); occipital WM was defined in the axial plane of the posterior CC, placed in the posterior portion of the WM within the occipital gyrus (Fig. 1a).

All regional definitions included only voxels with minimal partial voluming with CSF or gray matter. To further examine the potential influence of partial voluming, a number of thresholds were employed to exclude voxels with low FA values (values below .10, .15, .20, and .25). The exclusion of voxels with FA values below these thresholds was expected to remove voxels that were appreciably influenced by partial voluming. The results were not significantly altered with the application of these different thresholds, suggesting that partial volume effects were not a major determinant of the results. The higher end of these thresholds is conservative because the FA of CSF and cortical gray matter is typically below .2. Thus, we were conservative in excluding voxels with FA values below .2 in subsequent analyses.

2.6. Statistical analyses

We examined the ROI data using Pearson's correlation among all participants and by analysis of variance (ANOVA) among the YA, MA, and OA groups. Statistical values of $p \leq .01$ were considered statistically significant, and $p \leq .05$ were considered suggestive.

2.7. Whole brain maps

Additional group analyses examined the regional distribution of age-related reductions in FA. Spatially normalized FA maps were smoothed using a 3D spatial smoothing filter with a full width half maximum of 4 mm and compared by regression analysis (with age regressed as a continuous variable across each voxel in the volume), and by voxel based *t*-test across the three age groups. These analyses were considered exploratory because prior studies have noted the potential for misalignment in voxel-based volume registration, particularly for images where atrophy is expected. For example, age-related enlargement of the ventricular space results in an alteration of brain structure in older adults that partially confounds the ability to match white matter regions on a voxel-wise basis with younger adults. We sought to avoid such misregistration in several ways, including: (a) exclusion of all voxels considered CSF based on thresholding by the trace volume and excluding any voxel where a single participant did not contribute to the average (i.e., exclusion of any voxel that was trace masked in one or more participant's volumes to the analysis); (b) using mutual information procedures [25,26,53,54]; (c) interpreting only converging data from three complementary registration procedures (whole brain registration, WM registration, and fiducial landmark registration); (d) visual examination of each participant's transformed volume. Still, it is possible that misregistrations contribute to the presented results, and these maps are thus secondary to the ROI analyses. The a priori chosen ROIs support the findings of the whole brain analyses, lending confidence to these exploratory maps.

2.8. Diffusion tensormaps

Diffusion tensormaps were created for the qualitative examination of the WM fiber bundles most affected by aging. The diffusion tensor map is a three-dimensional rendering of the diffusion tensor data set, and provides information on the directional projection of large fiber bundles. A cuboid glyph at each voxel represents the local diffusion tensor. The axes of the cuboids are oriented in the direction of the diffusion tensor eigenvectors. The major axis of the cuboid gives the principal eigenvector of the diffusion tensor. The diffusion tensors are also colored according the direction of the principal eigenvector using a red–green–blue scheme with red indicating medial–lateral projecting fibers, green representing anterior–poster projecting fibers, and blue representing superior–inferior projecting fibers. Statistical effect maps were overlayed on the tensormap of a representative participant by reverse transform of the statistical map from standard space to the participant's native data space to avoid rotation of the tensor information.

3. Results

3.1. Regional analyses

FA values for the YA, MA, and OA participant groups were regionally variable (Table 3). WM regions with high degrees of myelination and homogeneous orientation, such as the CC and PLIC, had relatively high FA values, and more superficial and less structured regions, such as the

Table 3
Mean global and regional FA values in YA, MA, and OA

Region	YA[a] mean (S.D.)	MA[b] mean (S.D.)	OA[c] mean (S.D.)
Global	.40 (±.01)	.38 (±.01)	.37 (±.02)
Anterior CC[d]	.80 (±.07)	.74 (±.11)	.71 (±.09)
Posterior CC[d]	.83 (±.05)	.82 (±.07)	.80 (±.07)
PLIC[e]	.62/.59 (±.05/.04)	.56/.55 (±.05/.03)	.56/.53 (±.06/.06)
Deep frontal	.42/.46 (±.04/.05)	.38/.42 (±.09/.01)	.30/.36 (±.05/.06)
Anterior PV[f]	.32/.34 (±.05/.06)	.32/.32 (±.05/.04)	.29/.31 (±.06/.06)
Posterior PV[f]	.49/.51 (±.05/.05)	.45/.49 (±.05/.05)	.42/.45 (±.07/.07)
Medial orbitofrontal	.40/.42 (±.10/.10)	.36/.37 (±.08/.05)	.32/.32 (±.08/.09)
Inferior frontal	.40/.41 (±.09/.08)	.37/.40 (±.05/.07)	.35/.40 (±.05/.07)
Deep temporal	.41/.41 (±.07/.08)	.39/.40 (±.01/.07)	.38/.41 (±.01/.07)
Post-central	.30/.31 (±.06/.05)	.30/.31 (±.06/.05)	.31/.30 (±.06/.07)
Occipital	.31/.35 (±.07/.04)	.30/.33 (±.07/.06)	.31/.35 (±.10/.07)

Data presented for left/right hemisphere where applicable.
[a] YA: young adults.
[b] MA: middle-aged adults.
[c] OA: older adults.
[d] CC: corpus callosum.
[e] PLIC: posterior limb of the internal capsule.
[f] PV: periventricular.

subcortical WM of the inferior frontal gyrus, had relatively lower FA values. Scatterplots for the correlations between age and FA are presented in Figs. 2 (global) and 3 (regional). These analyses showed statistically significant reduction in FA with increasing age in the genu of the corpus callosum and bilaterally in the deep frontal, PLIC, medial orbitofrontal, and posterior periventricular ROIs. Similar results were obtained through ANOVA analyses among groups as described below.

ANOVA among YA, MA, and OA demonstrated significant effects globally $F(2, 35) = 18.2$, $p < .0001$; in the anterior CC $F(2, 35) = 3.6$, $p < .05$; the internal capsule bilaterally $F(2, 35) = 5.8$, $p < .01$; deep frontal WM bilaterally $F(2, 35) = 9.1$, $p < .001$; posterior periventricular WM bilaterally $F(2, 35) = 4.5$, $p < .01$; and in medial orbital WM bilaterally $F(2, 35) = 3.7$, $p < .05$ (Fig. 4). Post hoc testing using Fisher's PLSD showed that that OA had significantly lower FA globally ($p < .0001$), in the anterior CC ($p < .05$), deep frontal WM ($p < .001$), medial orbitofrontal WM ($p = .01$), PLIC ($p < .01$), and in posterior periventricular WM ($p < .01$). MA showed reduced FA globally ($p < .01$) and in the left and right PLIC ($p < .01$) compared to YA. There was a trend towards reduced FA in deep frontal WM of the left hemisphere ($p = .06$). Middle-aged adults had greater deep frontal FA bilaterally compared to OA ($p \leq .05$).

The finding of reduced FA in the PLIC was unexpected as it has been suggested that tissue associated with primary motor function is spared with aging. To examine this result further, we added two ROIs, one in the anterior limb of the internal capsule and an alternate ROI in the PLIC. These confirmatory ROIs were placed as a line of voxels down each limb in the axial view to disambiguate potential age-related changes in these different fiber systems. These alternate ROI analyses confirmed, and in fact strengthened, the significant decline in FA in the PLIC ($r = -.61$, $p < .0001$). In contrast, the anterior limb of the internal capsule was preserved with age ($r = -.06$, NS).

3.2. Whole brain maps

The exploratory whole brain analyses largely agreed with the findings reported from the ROI analyses (Fig. 5, top panel). Specifically, voxel-based regression of FA with age demonstrated regions of greatest decline were in the deep frontal WM, PLIC, and anterior CC. In contrast, temporal

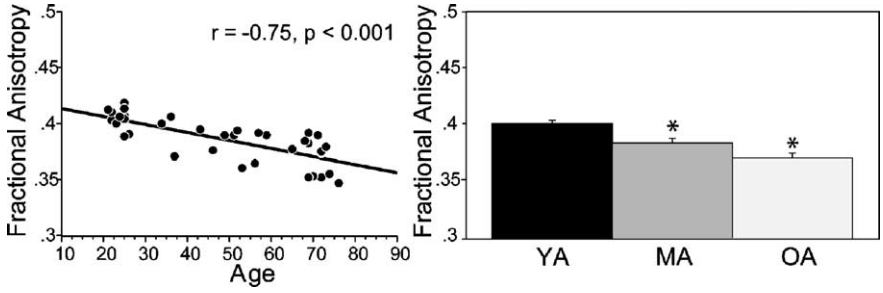

Fig. 2. Effect of aging on global FA. *Left panel*: Scatter plot of mean global FA regressed by age. Age significantly correlates with FA. *Right panel*: Mean FA in YA, MA, and OA. Bars represent mean and standard error of the mean (*$p < .01$).

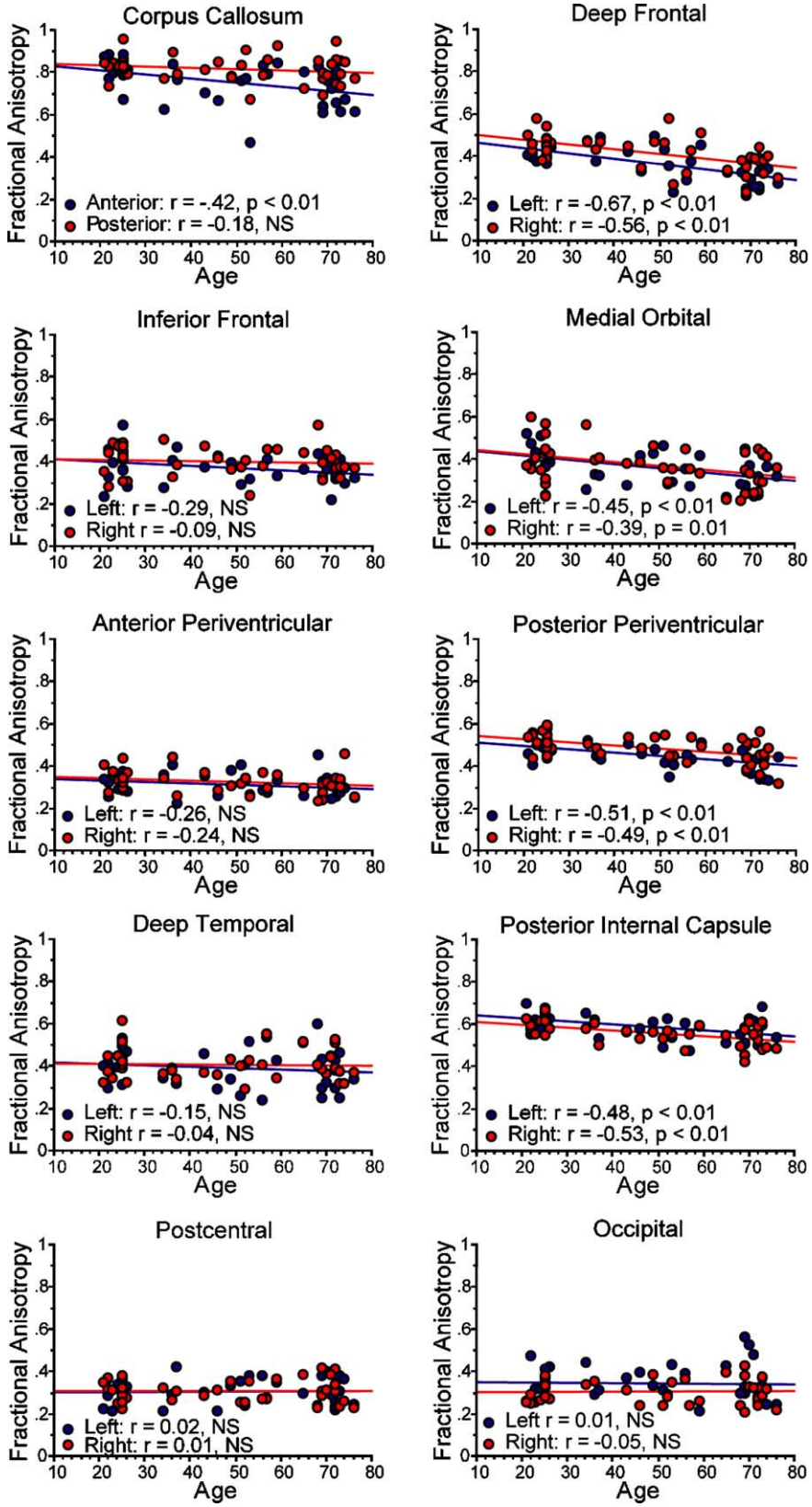

Fig. 3. Effect of aging on regional FA. Scatterplots of regional FA regressed by age as denoted by the regional demarcations above each plot and depicted in Fig. 1. Decline in FA was variable across brain WM with significant changes in the deep frontal, medial orbitofrontal, PLIC, and posterior periventricular ROIs. Relative preservation was found in a number of regions including temporal and occipital WM.

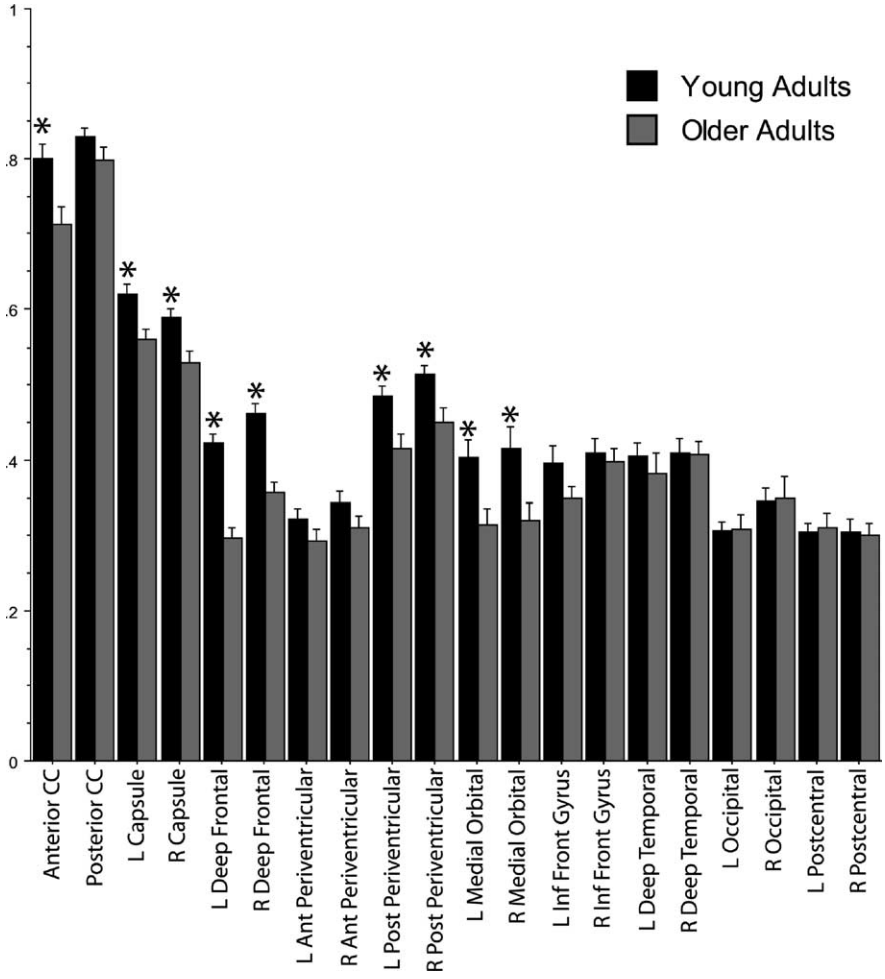

Fig. 4. Regional FA values in YA and OA. Regional measures of FA are presented for YA (black bars) and OA (gray bars). Regions were defined in each individual's low*b* volume as depicted in Fig. 1 and described in the text. Data are presented as the mean and S.E.M. for each region (*$p < .05$).

and more posterior WM was relatively spared. Statistical reductions in FA were regionally similar when examined as group voxel-based *t*-tests across the volume between the YA and OA, and when we used the three different registration procedures (whole brain, fiducial landmarks, and WM registration). These maps also suggested that statistical differences in FA were apparent by middle age (Fig. 5, bottom panel). Similar results were apparent when performing the analysis as a voxel-based regression with age across all participants (Fig. 6). The maps obtained were reliable in the regions of most pronounced reduction when splitting the sample into matched halves (a split of the sample matched for age and sex) and then running the same statistical analyses (Fig. 7).

4. Discussion

The current study demonstrated regionally selective age-related alterations in cerebral WM measured by FA. This effect was apparent globally, but was most notable in some prefrontal areas and the PLIC, and was not statistically significant in temporal and posterior regions of the brain. This finding suggests regional acceleration of WM degeneration with aging. Other findings, such as a greater decline in FA in the PLIC than in particular regions of frontal WM, imply that WM changes are not unique to prefrontal WM, and that these changes are regionally selective. In addition, although changes within the CC suggested an anterior to posterior gradient of change, other analyses are inconsistent with that conclusion, i.e., the significant alteration of posterior perventricular but not anterior periventricular WM, and regional preservation in some prefrontal WM. Rather, WM vulnerability seems to be conferred to particular fiber bundles, fiber populations, and regional locations. The group maps support the view that specific fiber bundles are affected with aging because portions of the statistical maps resemble known fiber anatomy and not non-anatomical areas of reduction. For example, a clear path of statistical significance is apparent in the pyramidal (corticospinal) tracts as revealed qualitatively by the location and shape of the statistical findings as well as the corresponding tensor data (Fig. 8).

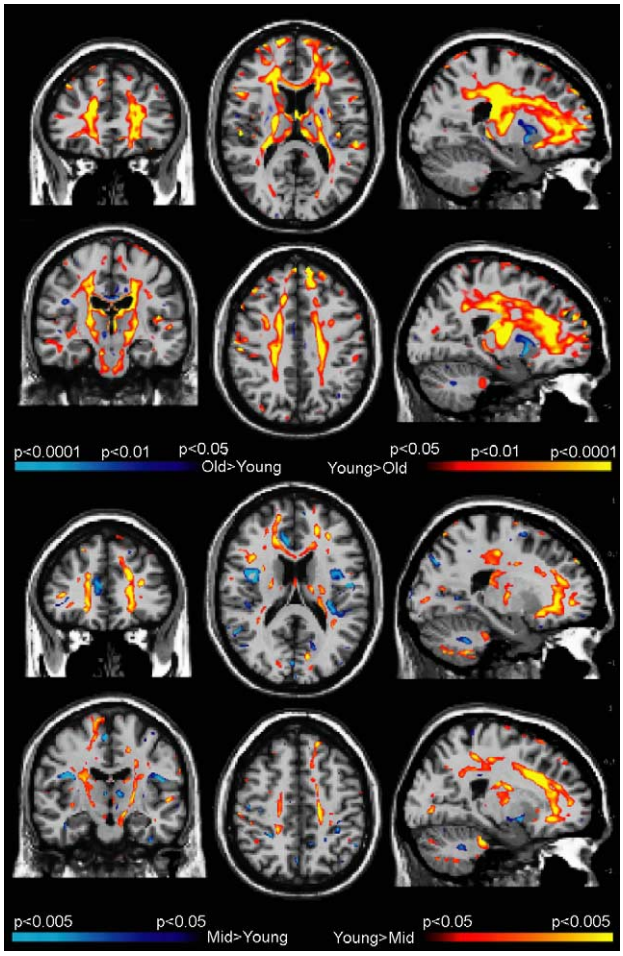

Fig. 5. *Top panel*: Map of age-related decline in FA in OA compared to YA. Voxel-based significance maps of FA decline with age computed by voxel level *t*-tests between the YA and OA groups. Maps are presented as three cardinal views in each hemisphere (top panel, left hemisphere; bottom panel, right hemisphere). The colorscale represents the significance of the age-related FA change, with yellow indicating regions of most significant decline. *Bottom panel*: Map of age-related decline in FA in middle-aged adults compared to young adults. Voxel-based significance maps of FA decline with age computed by voxel level *t*-tests between the YA and MA groups. Maps are presented as three cardinal views in each hemisphere (top panel, left hemisphere; bottom panel, right hemisphere). The colorscale represents the significance of the age-related FA change, with yellow indicating regions of most significant decline.

4.1. Relation to prior imaging and histological data

The present data are in agreement with prior imaging studies demonstrating age-related atrophy of prefrontal WM [51], greater frontal compared to temporal WM abnormalities [27], and marked reduction of FA in prefrontal WM [23,36]. Similarly, the data are also consistent with prior studies showing greater volume [18,49,62] and FA [40,59] reduction in anterior compared to posterior CC, and relative preservation of occipital WM [16]. One unexpected finding was the profound decline in FA in the PLIC. This finding was strengthened by using an additional ROI created with an alternative anatomical definition (the spherical ROI in the coronal orientation

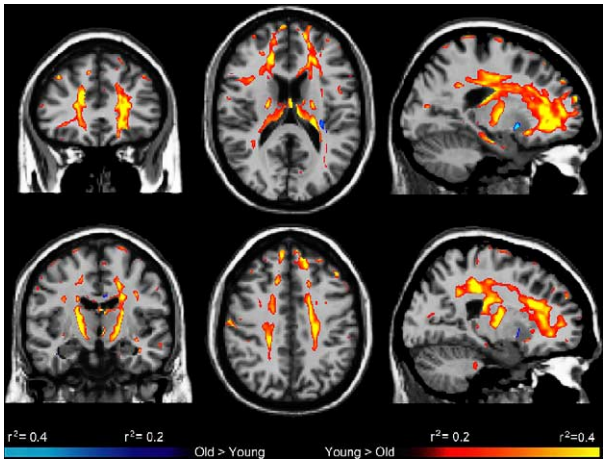

Fig. 6. Voxel-based regression of FA with age across all participants. Maps are presented as *r*-squared values in three cardinal views (top panel, left hemisphere; bottom panel, right hemisphere).

for the first definition, and a line down the PLIC in the axial orientation the second definition). The exploratory whole brain maps and ROI analyses suggest that changes in this region are apparent by middle age. We hypothesized that the corticospinal tracts would be relatively spared with aging because theories of brain aging suggest a sparing of primary sensory and motor cortices and their associated WM relative to association cortices. The whole brain group maps support the regional findings and suggest that changes occur through a large extent of the corticospinal pathway. Prior histological work described an age-related reduction in the number of myelinated fibers of spinal WM [61]. Additionally, recent work demonstrated significant age-related thinning of cortical tissue in the precentral gyrus [50], where these corticospinal fibers are expected to originate. The particular selection of regional WM ROIs in this study allows for more

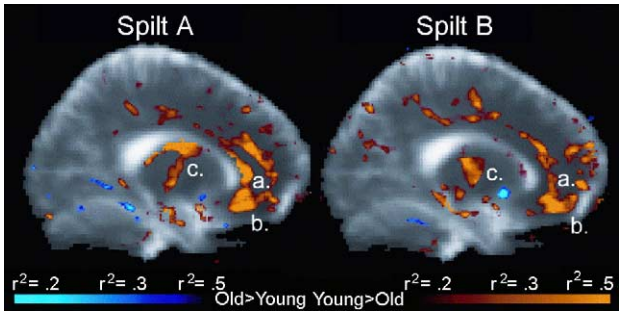

Fig. 7. Split sample reliability of maps of age-related FA reduction. Statistical maps of age-related reduction in FA are presented for two independent samples of participants comprising age and sex-matched splits of the total sample. Differences between samples can be detected; yet, the regions showing most prominent decline in FA in regional measurements and total sample group maps are similar between the independent samples, suggesting reliability in the volume maps. Specifically, large regions of reduction were found in (a) deep frontal, (b) medial orbitofrontal, and (c) PLIC WM. The correspondence between the volume maps and the ROI measurements suggests validity of the group maps.

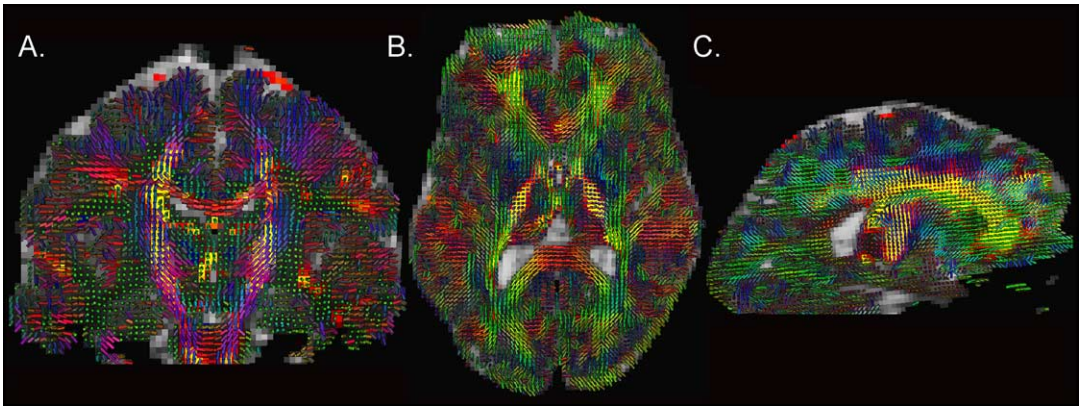

Fig. 8. Qualitative assessment of age-related decline in FA localized to the pyramidal tracts through use of a diffusion tensor map. Statistical results were registered and overlayed on the tensor maps of a representative individual participant. Age-related reduction in FA qualitatively resembled anatomically relevant structure, as opposed to less structured regions, suggesting that the observed results correspond to specific WM fiber bundles. The cubes depict the diffusion tensor within each voxel. The axes of each cube are oriented in the direction of the principal eigenvector of the local diffusion tensor. The cubes are colored by the direction of the principal eigenvector with red indicating mediolateral fibers (e.g., CC), green indicating anteroposterior fibers (e.g., superior longitudinal fasciculus), and blue indicating superoinferior fibers (e.g., PLIC) in the (A) coronal plane, (B) axial plane, and (C) sagittal plane.

anatomically specific hypotheses about the fiber populations most susceptible to age related degeneration. For example, preservation of the anterior limb of the internal capsule with age-related reduction in FA in the genu of the corpus callosum suggests that the frontal lobe fibers most affected are those of the forceps minor (as opposed to the frontothalamic or frontopontine fibers). Thus, the current data support a selective vulnerability of specific anterior fiber bundles, in particular, fibers within the prefrontal WM, anterior callosal fibers, and the corticospinal tracts.

An interesting exception to the anterior to posterior gradient of WM alteration comes from the finding that posterior periventricular regions show a greater decline in FA than anterior periventricular regions. Periventricular WM abnormalities are often reported with aging, although few studies have described the regional selectivity of such changes. Our data suggest that periventricular changes are not uniform, and that a linear decline in WM integrity occurs in the posterior regions. WM hypointensites were minimal in this participant population; yet, there was no attempt to avoid WM hypointensites from regional ROI placement. The effect of hypointensities on FA measures was minimal as assessed by thresholding each ROI for low FA values. Additionally, standard measurements of WM hypointensities in the literature refer to their presence or absence, as opposed to grading the amount of alteration in signal intensity, because such regions are usually quite different in signal intensity compared to surrounding tissue. This could be expected to result in a more catastrophic effect of age as opposed to the linear changes found in FA in this study. Hypointensities have been described as having a non-specific pathological origin [3] and to not be strongly related to cognitive abilities [55]. Thus, it is possible that the linear changes measured through DTI could represent a more specific and clinically relevant aspect of WM pathology.

The histopathological origins of age-related WM degeneration are varied. Prior studies suggest that WM damage is primarily related to ischemic events because of small vessel changes [39]. Consequently, WM changes are related to hypertension [52]. Additional pathological correlates include gliosis [20,60] and decreases in myelinated axons [9,35]. Other notable age-related changes in WM, such as lacunar infarcts, likely do not contribute to the changes observed in the present study because these participants were free from such apparent lesions on their conventional MR images (although we cannot exclude the possibility of similar physiological changes below the resolution of conventional MR). Still, the true nature of the tissue alterations underlying changes in FA is currently unknown, and an important developing application of DTI is the ex vivo histopathological characterization of regional changes measured in vivo.

4.2. Diffusion tensor imaging

Age-related degenerative changes in WM have been documented using various histological and imaging procedures [9,35]. A continuing challenge is to bridge commonly measured morphological changes, such as atrophy, with their histological correlates. This need is especially true given the heterogeneous nature of WM myeloarchitecture and pathology. Diffusion anisotropy [6] and related MR signal measures [16] provide a metric of tissue characteristics [6] that could ultimately represent a microstructural basis of volumetric measurements. Thus, these techniques represent a potential link between the MR and histological domains, and future studies will examine the relationship between age-related reductions volumetric, histological, and anisotropy measures. Such studies will be important as few studies have attempted to examine the biophysical basis of WM anisotropy, and few if any have described how changes in FA relate to specific aspects of

tissue pathology. More advanced applications for diffusion tensor data, such as tensor mapping and tractography techniques, are a promising lead towards understanding normal and abnormal anatomy. Fig. 8 demonstrates a descriptive use of a tensor map, showing that a statistical reduction in FA overlaps the tensor map representing the PLIC, providing support that the changes are path specific. Still, such techniques currently allow only for qualitative description and more quantitative analyses of tensor data will be necessary to precisely identify vulnerable pathways. Further development of these techniques will be essential towards this task.

4.3. Prefrontal WM

Age-related changes in the prefrontal cortex are believed to play a major role in age-related cognitive decline. Neuroimaging studies demonstrate that this region of the brain shows numerous age-related changes including accelerated cortical atrophy [45]. Prefrontal WM atrophy has also been reported with aging [28,45,51]; yet, the regional distribution of WM degeneration within the prefrontal cortex has not been described. The present study suggests that prefrontal WM changes are significant, but regionally selective. Older adults had significantly reduced FA in deep frontal and medial orbitofrontal WM, but not inferior frontal WM compared to young adults. Several functional neuroimaging studies have now documented age-related deviations in patterns of brain activation (e.g., [10,11,15,57,58]). Understanding patterns of WM degeneration will be critical towards determining how age-related structural brain changes contribute to abnormalities measured by functional neuroimaging.

4.4. Limitations and future directions

The limitations in the present study are now being addressed in ongoing work. First, although a balanced echo sequence was employed to reduce eddy current distortion and post-processing was used to reduce residual distortion and motion, echo-planar scans are susceptible to additional distortions including reduced signal in susceptibility regions of the brain [29]. Analyses were limited to regions of deep WM in an attempt to avoid this limitation. We found significant change in one susceptibility region (medial orbitofrontal WM), suggesting that this susceptibility did not prevent us from detecting statistical effects. Still, development of DTI sequences with less susceptibility-related distortions would be advantageous for addressing this potential drawback (e.g., [2]). Additionally, such sequences would be useful for more accurate spatial transformation of DTI volumes across participants for whole brain group maps. The regional measurements are limited in that they sample only a small portion of the entire region. That is, although the regions of parietal, temporal, and occipital WM sampled for this study were spared, other regions (or fiber bundles) within these lobes could be affected by aging. Future studies will examine regions of degeneration and preservation in more detail to determine the full extent of such patterns in the regions noted. Finally, all studies of regional brain differences in structure or function are likely influenced by regional sensitivity to the measures employed, based both on the biology and the analysis technique. In the present study, it is likely that the biological homogeneity of a particular ROI determined the power to detect statistical differences in a specific fiber population between groups. For this reason, regions of higher FA could provide greater statistical power. The data demonstrate that we were able to detect statistical change as well as preservation in regions of high and low FA, suggesting that the native FA value of a particular region in young adults does not greatly affect the ability to detect statistical changes in this study. Future studies will incorporate tensor data into the regional definitions to reduce the potential impact of these concerns. In spite of these limitations, our data strongly support the idea of preferential vulnerability in specific fiber systems within the frontal lobe and PLIC to age-related degeneration.

Acknowledgements

This work was supported by AG05886, HBP:NS39581 and RR14075, the NCRR P41:RR14075, the Mental Illness and Neuroscience Discovery (MIND) Institute, AG14432, Glaxo Smith Kline, and through a pilot grant from the Massachusetts Alzheimer's Disease Research Center 5:P50:AG05134. The authors thank Richard Clarke, Mette Wiegell, Thomas Benner, Tim Reese, and Kevin Teich for assistance in the development of these projects.

References

[1] Ardekani BA, Nierenberg J, Hoptman MJ, Javitt DC, Lim KO. MRI study of white matter diffusion anisotropy in schizophrenia. Neuroreport 2003;14(16):2025–9.
[2] Bammer R, Auer M, Keeling SL, et al. Diffusion tensor imaging using single-shot SENSE-EPI. Magn Reson Med 2002;48(1):128–36.
[3] Barkhof F, Scheltens P. Imaging of white matter lesions. Cerebrovasc Dis 2002;13(Suppl. 2):21–30.
[4] Bartzokis G, Cummings JL, Sultzer D, Henderson VW, Nuechterlein KH, Mintz J. White matter structural integrity in healthy aging adults and patients with Alzheimer disease: a magnetic resonance imaging study. Arch Neurol 2003;60(3):393–8.
[5] Basser PJ, Mattiello J, LeBihan D. Estimation of the effective self-diffusion tensor from the NMR spin echo. J Magn Reson B 1994;103(3):247–54.
[6] Beaulieu C. The basis of anisotropic water diffusion in the nervous system—a technical review. NMR Biomed 2002;15(7–8):435–55.
[7] Bozzali M, Franceschi M, Falini A, et al. Quantification of tissue damage in AD using diffusion tensor and magnetization transfer MRI. Neurology 2001;57(6):1135–7.
[8] Brandt J, Welsh KA, Breitner JC, Folstein MF, Helms M, Christian JC. Hereditary influences on cognitive functioning in older men. A study of 4000 twin pairs. Arch Neurol 1993;50(6):599–603.
[9] Bronge L, Bogdanovic N, Wahlund LO. Postmortem MRI and histopathology of white matter changes in Alzheimer brains. A quantitative, comparative study. Dement Geriatr Cogn Disord 2002;13(4):205–12.

[10] Buckner RL, Snyder AZ, Sanders AL, Raichle ME, Morris JC. Functional brain imaging of young, nondemented, and demented older adults. J Cogn Neurosci 2000;12(Suppl. 2):24–34.
[11] Cabeza R, Anderson ND, Locantore JK, McIntosh AR. Aging gracefully: compensatory brain activity in high-performing older adults. Neuroimage 2002;17(3):1394–402.
[12] Christiansen P, Larsson HB, Thomsen C, Wieslander SB, Henriksen O. Age dependent white matter lesions and brain volume changes in healthy volunteers. Acta Radiol 1994;35(2):117–22.
[13] Ciccarelli O, Werring DJ, Barker GJ, et al. A study of the mechanisms of normal-appearing white matter damage in multiple sclerosis using diffusion tensor imaging—evidence of Wallerian degeneration. J Neurol 2003;250(3):287–92.
[14] Cowell PE, Turetsky BI, Gur RC, Grossman RI, Shtasel DL, Gur RE. Sex differences in aging of the human frontal and temporal lobes. J Neurosci 1994;14(8):4748–55.
[15] D'Esposito M, Zarahn E, Aguirre GK, Rypma B. The effect of normal aging on the coupling of neural activity to the bold hemodynamic response. Neuroimage 1999;10(1):6–14.
[16] Davatzikos C, Resnick SM. Degenerative age changes in white matter connectivity visualized in vivo using magnetic resonance imaging. Cereb Cortex 2002;12(7):767–71.
[17] de Jager CA, Budge MM, Clarke R. Utility of TICS-M for the assessment of cognitive function in older adults. Int J Geriatr Psychiatry 2003;18(4):318–24.
[18] Doraiswamy PM, Figiel GS, Husain MM, McDonald WM, Shah SA, Boyko OB, et al. Aging of the human corpus callosum: magnetic resonance imaging in normal volunteers. J Neuropsychiatry Clin Neurosci 1991;3(4):392–7.
[19] Folstein MF, Folstein SE, McHugh PR. Mini-mental state: a practical method for grading the state of patients for the clinican. J Psychiatr Res 1975;12:189–98.
[20] Grafton ST, Sumi SM, Stimac GK, Alvord Jr EC, Shaw CM, Nochlin D. Comparison of postmortem magnetic resonance imaging and neuropathologic findings in the cerebral white matter. Arch Neurol 1991;48(3):293–8.
[21] Guo AC, Jewells VL, Provenzale JM. Analysis of normal-appearing white matter in multiple sclerosis: comparison of diffusion tensor MR imaging and magnetization transfer imaging. AJNR Am J Neuroradiol 2001;22(10):1893–900.
[22] Guttmann CR, Jolesz FA, Kikinis R, Killiany RJ, Moss MB, Sandor T, et al. White matter changes with normal aging. Neurology 1998;50(4):972–8.
[23] Head D, Buckner RL, Shimony JS, Williams LE, Akbudak E, Conturo TE, et al. Differential vulnerability of anterior white matter in nondemented aging with minimal acceleration in dementia of the Alzheimer type: evidence from diffusion tensor imaging. Cereb Cortex 2004;14(4):410–23.
[24] Hoptman MJ, Volavka J, Johnson G, Weiss E, Bilder RM, Lim KO. Frontal white matter microstructure, aggression, and impulsivity in men with schizophrenia: a preliminary study. Biol Psychiatry 2002;52(1):9–14.
[25] Jenkinson M, Bannister P, Brady M, Smith S. Improved optimization for the robust and accurate linear registration and motion correction of brain images. Neuroimage 2002;17(2):825–41.
[26] Jenkinson M, Smith S. A global optimisation method for robust affine registration of brain images. Med Image Anal 2001;5(2):143–56.
[27] Jernigan TL, Archibald SL, Berhow MT, Sowell ER, Foster DS, Hesselink JR. Cerebral structure on MRI. Part I: localization of age-related changes. Biol Psychiatry 1991;29(1):55–67.
[28] Jernigan TL, Archibald SL, Fennema-Notestine C, et al. Effects of age on tissues and regions of the cerebrum and cerebellum. Neurobiol Aging 2001;22(4):581–94.
[29] Jezzard P, Clare S. Sources of distortion in functional MRI data. Hum Brain Mapp 1999;8(2–3):80–5.
[30] Kemper TL. Neuroanatomical and neuropathological changes during aging and in dementia. In: Albert ML, Knoepfel EJE, editors. Clinical neurology of aging. 2nd ed. New York: Oxford University Press; 1994. p. 3–67.
[31] Kubicki M, Westin CF, Maier SE, et al. Uncinate fasciculus findings in schizophrenia: a magnetic resonance diffusion tensor imaging study. Am J Psychiatry 2002;159(5):813–20.
[32] Lim KO, Hedehus M, Moseley M, de Crespigny A, Sullivan EV, Pfefferbaum A. Compromised white matter tract integrity in schizophrenia inferred from diffusion tensor imaging. Arch Gen Psychiatry 1999;56(4):367–74.
[33] Lim KO, Helpern JA. Neuropsychiatric applications of DTI—a review. NMR Biomed 2002;15(7–8):587–93.
[34] Lipton RB, Katz MJ, Kuslansky G, et al. Screening for dementia by telephone using the memory impairment screen. J Am Geriatr Soc 2003;51(10):1382–90.
[35] Meier-Ruge W, Ulrich J, Bruhlmann M, Meier E. Age-related white matter atrophy in the human brain. Ann N Y Acad Sci 1992;673:260–9.
[36] Nusbaum AO, Tang CY, Buchsbaum MS, Wei TC, Atlas SW. Regional and global changes in cerebral diffusion with normal aging. AJNR Am J Neuroradiol 2001;22(1):136–42.
[37] O'Sullivan M, Jones DK, Summers PE, Morris RG, Williams SC, Markus HS. Evidence for cortical "disconnection" as a mechanism of age-related cognitive decline. Neurology 2001;57(4):632–8.
[38] Ostergaard L, Sorensen AG, Chesler DA, et al. Combined diffusion-weighted and perfusion-weighted flow heterogeneity magnetic resonance imaging in acute stroke. Stroke 2000;31(5):1097–103.
[39] Pantoni L. Pathophysiology of age-related cerebral white matter changes. Cerebrovasc Dis 2002;13(Suppl. 2):7–10.
[40] Pfefferbaum A, Sullivan EV. Increased brain white matter diffusivity in normal adult aging: Relationship to anisotropy and partial voluming. Magn Reson Med 2003;49(5):953–61.
[41] Pfefferbaum A, Sullivan EV, Hedehus M, Adalsteinsson E, Lim KO, Moseley M. In vivo detection and functional correlates of white matter microstructural disruption in chronic alcoholism. Alcohol Clin Exp Res 2000;24(8):1214–21.
[42] Pfefferbaum A, Sullivan EV, Hedehus M, Lim KO, Adalsteinsson E, Moseley M. Age-related decline in brain white matter anisotropy measured with spatially corrected echo-planar diffusion tensor imaging. Magn Reson Med 2000;44(2):259–68.
[43] Pierpaoli C, Basser PJ. Toward a quantitative assessment of diffusion anisotropy. Magn Reson Med 1996;36(6):893–906.
[44] Raz N. Aging of the brain and its impact on cognitive performance: integration of structural and functional findings. In: Craik FIM, Salthouse TA, editors. Handbook of aging and cognition—II. Hillsdale: Erlbaum; 2000. p. 1–90.
[45] Raz N, Gunning FM, Head D, et al. Selective aging of the human cerebral cortex observed in vivo: differential vulnerability of the prefrontal gray matter. Cereb Cortex 1997;7(3):268–82.
[46] Reese TG, Heid O, Weisskoff RM, Wedeen VJ. Reduction of eddy-current-induced distortion in diffusion MRI using a twice-refocused spin echo. Magn Reson Med 2003;49(1):177–82.
[47] Resnick SM, Pham DL, Kraut MA, Zonderman AB, Davatzikos C. Longitudinal magnetic resonance imaging studies of older adults: a shrinking brain. J Neurosci 2003;23(8):3295–301.
[48] Rovaris M, Iannucci G, Falautano M, et al. Cognitive dysfunction in patients with mildly disabling relapsing–remitting multiple sclerosis: an exploratory study with diffusion tensor MR imaging. J Neurol Sci 2002;195(2):103–9.
[49] Salat D, Ward A, Kaye JA, Janowsky JS. Sex differences in the corpus callosum with aging. Neurobiol Aging 1997;18(2):191–7.
[50] Salat DH, Buckner RL, Snyder AZ, Greve DN, Desikan RS, Busa E, Morris JC, et al. Thinning of the cerebral cortex in aging. Cereb Cortex 2004;14(7):721–30.

[51] Salat DH, Kaye JA, Janowsky JS. Prefrontal gray and white matter volumes in healthy aging and Alzheimer disease. Arch Neurol 1999;56(3):338–44.
[52] Skoog I. A review on blood pressure and ischaemic white matter lesions. Dement Geriatr Cogn Disord 1998;9(Suppl. 1):13–9.
[53] Smith SM, De Stefano N, Jenkinson M, Matthews PM. Normalized accurate measurement of longitudinal brain change. J Comput Assist Tomogr 2001;25(3):466–75.
[54] Smith SM, Zhang Y, Jenkinson M, et al. Accurate, robust, and automated longitudinal and cross-sectional brain change analysis. Neuroimage 2002;17(1):479–89.
[55] Soderlund H, Nyberg L, Adolfsson R, Nilsson LG, Launer LJ. High prevalence of white matter hyperintensities in normal aging: relation to blood pressure and cognition. Cortex 2003;39(4–5):1093–105.
[56] Sorensen AG, Copen WA, Ostergaard L, et al. Hyperacute stroke: simultaneous measurement of relative cerebral blood volume, relative cerebral blood flow, and mean tissue transit time. Radiology 1999;210(2):519–27.
[57] Sperling RA, Bates JF, Chua EF, et al. fMRI studies of associative encoding in young and elderly controls and mild Alzheimer's disease. J Neurol Neurosurg Psychiatry 2003;74(1):44–50.
[58] Stebbins GT, Carrillo MC, Dorfman J, Dirksen C, Desmond JE, Turner DA, et al. Aging effects on memory encoding in the frontal lobes. Psychol Aging 2002;17(1):44–55.
[59] Sullivan EV, Adalsteinsson E, Hedehus M, et al. Equivalent disruption of regional white matter microstructure in ageing healthy men and women. Neuroreport 2001;12(1):99–104.
[60] Takao M, Koto A, Tanahashi N, Fukuuchi Y, Takagi M, Morinaga S. Pathologic findings of silent hyperintense white matter lesions on MRI. J Neurol Sci 1999;167(2):127–31.
[61] Terao S, Sobue G, Hashizume Y, Shimada N, Mitsuma T. Age-related changes of the myelinated fibers in the human corticospinal tract: a quantitative analysis. Acta Neuropathol (Berl) 1994;88(2):137–42.
[62] Weis S, Kimbacher M, Wenger E, Neuhold A. Morphometric analysis of the corpus callosum using MR: correlation of measurements with aging in healthy individuals. AJNR Am J Neuroradiol 1993;14(3):637–45.
[63] Werring DJ, Clark CA, Barker GJ, Thompson AJ, Miller DH. Diffusion tensor imaging of lesions and normal-appearing white matter in multiple sclerosis. Neurology 1999;52(8):1626–32.
[64] Wolkin A, Choi SJ, Szilagyi S, Sanfilipo M, Rotrosen JP, Lim KO. Inferior frontal white matter anisotropy and negative symptoms of schizophrenia: a diffusion tensor imaging study. Am J Psychiatry 2003;160(3):572–4.
[65] Wu O, Koroshetz WJ, Ostergaard L, et al. Predicting tissue outcome in acute human cerebral ischemia using combined diffusion- and perfusion-weighted MR imaging. Stroke 2001;32(4):933–42.